# *Data report*

## *Hydrodynamics and sediment dynamics Mandai Mangrove, Singapore*
## *10/02/2015 – 05/05/2015*

Part of Master Thesis

## P. W. J. M. Willemsen

University of Twente
National University of Singapore

UT supervisor:           Dr. ir. C. M. Dohmen-Janssen
UT daily supervisor:     Dr. ir. B. W. Borsje
UT daily supervisor:     Dr. ir. E. M. Horstman
NUS daily supervisor:    Dr. D. Friess

# Contents

# 1. INTRODUCTION

Coastal wetlands are unique ecosystems, located at the interface between land and sea where they provide a great range of livelihood and regulating services, e.g. coastal protection due to wave attenuation and coastal stabilization, providing wood and food, increasing water quality and the assimilation of carbon (Robertson et al. 1992; Hong et al. 1993; Hsiang 2000; Mazda et al. 2007). The value of these ecosystem services is estimated at $12.000 per hectare per year (de Groot et al. 2012), making it one of the most valuable ecosystems globally and the most valuable coastal landform (Costanza et al. 1998). Coastal wetlands thrive in the quiescent intertidal areas of estuaries, deltas, backwater areas, and lagoons and are (more specified) mangroves at tropical and sub-tropical latitudes (Mazda et al. 2007). In contradiction to their value, worldwide mangroves are vulnerable and highly threatened tropical environments (Kirwan et al. 2013). With an average area loss of 2.1% per year since the early 1980s, mangrove losses exceed those of tropical rain forests and coral reefs (Valiela et al. 2001). Besides natural forces, mangroves are under an immense anthropogenic pressure, which is still increasing (Friess et al. 2012). Human activities, e.g. industrialisation, urbanization, mariculture / aquaculture, etc. contributes to these losses (Wolanski et al. 2000; Valiela et al. 2001; Friess et al. 2012). Also indirect anthropogenic influences affect mangroves, e.g. chemical spill and sea level rise (SLR), as well as decreased sediment delivery rates (Thampanya et al. 2006; Kirwan et al. 2013). Globally, large reservoirs trap 20% of the total terrestrial sediment flux, in addition small reservoirs trap another 6% that never reaches the coastal system (Syvitski et al. 2005).

Knowledge of the biophysical resilience of natural mangroves has been developed by studies of e.g. Thampanya et al. (2006), Horstman et al. (2015) and Van Maanen et al. (2015). Natural mangroves can cope with (in)direct anthropogenic influences e.g. a certain amount of sea level rise and a decreased sediment influx, until a species-specified threshold to tidal inundation is reached (Friess et al. 2012). However, (in)direct human impacts on mangroves interact with each other and with SLR. Hence incorporating the indirect effects of human activity on inter alia sediment availability, into biophysical models of coastal wetland evolution is an important challenge that has not yet been addressed (Kirwan et al. 2013).

To address this challenge a derivative from the Singapore Regional Model (SRM) (Kernkamp et al. 2005; Kurniawan et al. 2011; Hasan et al. 2012), is used to develop a model for the anthropogenic influenced Mandai mangrove in Singapore. For calibrating this model and getting insights in the hydrodynamics and sediment dynamics of mangroves under anthropogenic pressure, data is collected in Mandai mangrove. Flow velocities are collected as well as water levels, in addition to these hydrodynamics, vegetation data is collected to expand the current knowledge (Lee 2014). Suspended sediment concentrations, sediment deposition, grain size characteristics and organic matter content are measured and analysed. The different measurements are described in this data report.

## 1.1. STUDY SITE

The study site is located in Singapore (Fig. 1A) at Mandai mangrove (Fig. 1). (1°26'21''N; 103°45'49''E), which is located in northern Singapore, enclosed by the former Singapore-Malaysia railway, the Straits of Johor and bordered by the rivers Sungei Mandai and Sungei Mandai Kechil, at the southwestern and northeastern side respectively (Fig. 1). Mandai mangrove covers approximately 15.4 ha (Yee et al. 2010) and was once part of an extensive mangrove forest along the Singapore coast. Remnants of these extensive mangroves can still be found in Sungei Buloh Wetland Reserve and in some other parks along the north shores of Singapore. Anthropogenic influences are showed by the blocked tidal exchange due to the construction of the Johor causeway in 1913 (Friess et al. 2012), the fixed boundary at the back of the mangrove by the former Singapore-Malaysia railway, suppressing landward development. Finally the Kranji dam is constructed blocking a source of sediment at the western side of Mandai mangrove (Fig. 1B).
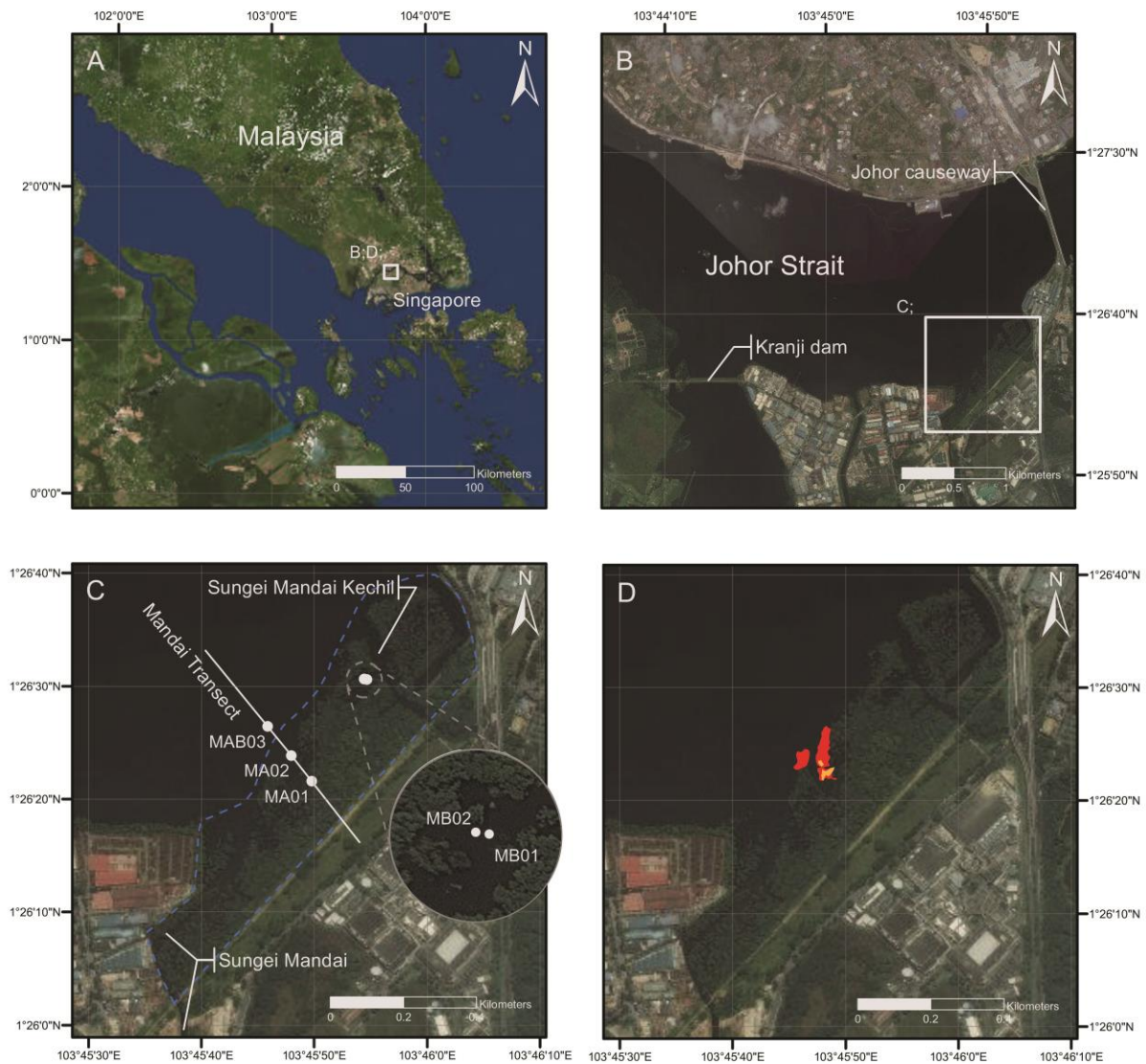
*FIGURE 1. (A) SINGAPORE AND SOUTHERN MALAYSIA SURROUNDED BY THE MALACCA STRAIT, SINGAPORE STRAIT AND THE SOUTH CHINA SEA. (B) THE STRAITS OF JOHOR WITH THE ADJACENT MANDAI MANGROVE. (C) MANDAI MANGROVE INCLUDING MEASUREMENT LOCATIONS AND MANGROVE EXTENT (BLUE BORDER). (D) LOCATIONS OF VEGETATION MEASUREMENTS.*

## 1.2. MEASUREMENT LOCATIONS

Five locations are chosen to conduct the measurements, due to the restricting amount of only 3 pieces of measurement equipment, this is the maximum amount of locations. Three measurement locations are situated at the Mandai transect, two additional locations, for getting a full picture of all locations with different characteristics, are added. The locations (Fig. 1C) are chosen taking the following criteria into account:

- The transect should consist a mud flat in front of the forest, a forest fringe and an inner mangrove part (Horstman 2014), which should all be convincingly flooded (more than 0.25m, because of the equipment) during spring tide.
- The vegetation density should increase from the mud flat (front of the mangrove forest) to the inner part of the mangrove forest.
- The mangrove should be homogeneous around the measurement locations, i.e. there should not be any rivers, tidal creeks, sudden elevation changes or other disturbances around the areas where the equipment is deployed.
- The vegetation density at the measurement locations should not be too dense, i.e. the additional flow and eddies created by the vegetation should not disturb the measurements.

- The bottom should be suitable for inserting (bamboo) canes for mounting the ADVs.

All locations are described below:
- MA01: relative dense forest at the back of the mangrove (Fig. 2A).
- MA02: a patch with *Sonneratia* saplings (Fig. 2B).
- MAB03: the mudflat in front of the mangrove, with an algae film on top (Fig. 2C). This location is present at both transects and used as a reference location.
- MB02: bank of a tidal creek, which is not exposed to a layer of water during low tide (Fig. 2D).
- MB01: tidal creek, which is exposed to a layer of water during low tide (Fig. 2D).

The first day of a measurement period the locations at the Mandai transect (Fig. 1C) are used for conducting measurements and the second day the locations MB01, MB02 and MAB03 (Fig. 1C) are used for conducting measurements



FIGURE 2. MEASUREMENT LOCATIONS, FROM TOP LEFT TO BOTTOM RIGHT: MA01 (A), MA02 (B), MAB03 (C), MB02 AND MB01 (D).

# 2. METHODS FOR MEASURING

Different measurements are conducted at the measurement locations, this includes: sediment deposition, grain size characteristics, organic matter content, suspended sediment concentrations (SSCs), water levels and flow velocities. The measurements are executed during two periods: 24-25 March 2015 and 5-7 April 2015. In addition vegetation characteristics are measured in representative plots around measurement location MA02.

## 2.1. VEGETATION

The locations where recently new vegetation made its appearance are collected using a Garmin GPSMAP 62s. A waypoint is collected every 10 steps (Fig. 3). *Sonneratia* saplings are sampled within one plot with a radius of 7m. *Sonneratia* saplings (Fig. 4) with a stem diameter (at the bottom) above 1cm or higher than 70cm are included in the measurements. The circumference at the bottom is measured (for calculating the diameter), the largest diameter is measured (including branches and leafs), the total height as well as the height of the first split of the stem is measured and the circumference of the branches at the first split is measured (for calculating the diameter). Five representative *Sonneratia* trees (Fig. 4) are measured as well. The circumference at the bottom is measured (for calculating the diameter), the diameter at breast height (DBH), i.e. at 150 cm) is measured as well as the largest diameter (including branches and leafs) below DBH. The largest diameter below DBH is measured, because that part is exposed to high tide and subsequently creates the roughness. The amount of *Sonneratia* trees in the northern and southern patch (Fig. 3) is counted and can be represented by the sampled trees.
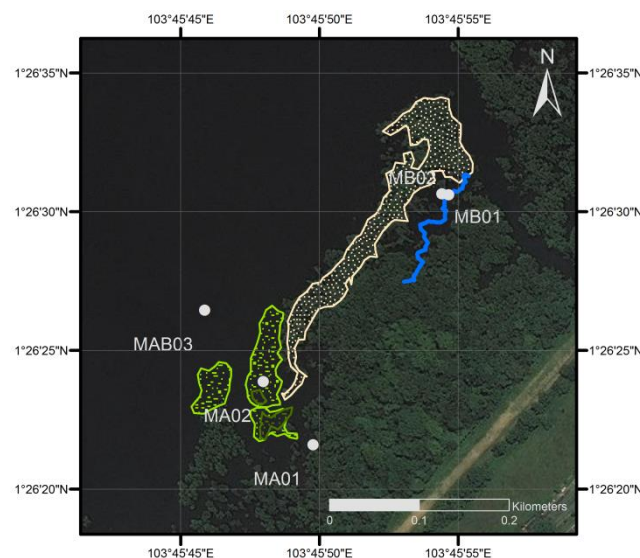


**FIGURE 3. PATCHES OF *SONNERATIA* VEGETATION SHOWING *SONNERATIA* TREES (DARK GREEN) AND *SONNERATIA* SAPLINGS (LIGHT GREEN). THE DIFFERENT MEASUREMENT LOCATIONS ARE LABELED AND SHOWED WITH GRAY DOTS, AS WELL AS THE SANDBANK (LIGH BROWN) AND THE TIDAL CREEK RELATED TO THE MEASUREMENT LOCATIONS MB01 AND MB02.**

**FIGURE 4. VEGETATION DATA COLLECTION CAPTURED, FROM LEFT TO RIGHT: MARKED *SONNERATIA* SAPPLING AFTER MEASURING (A), *SONNERATIA* TREES IN PATCHES OF *SONNERATIA* SHRUBS (B).**

## 2.2.    SEDIMENT DEPOSITION

The deposited sediment is measured with sediment traps. Different designs are tested: canvas sediment traps (based on e.g. Van Santen et al. (2007)) and sediment traps from acrylic glass of different sizes.  The canvas sediment traps were 0.4m x 0.4m and consists of a sheet canvas with a sheet of plastic at the bottom side. The structure/roughness on top of the canvas visually approached the roughness of the muddy mangrove bottom. The sediment trap was mounted using 4 metal pins putted through iron holes at the vertices of the canvas trap (Fig. 5A). The plastic cover was for protecting the bottom part of the canvas trap from sediment and was removed after the measurements were finished.  During testing this design it was noticed that the centre part of the trap was bulging (Fig. 5B). The sediment deposited on the trap was rinsed using distilled water and filtered. A second design consists of sheets from acrylic glass with different sizes, roughened with sandpaper. Sheets from 0.15m x 0.15m and sheets from 0.20m x 0.20m were systematically roughened using sandpaper with three different grain sizes starting with sandpaper with the finest grain size. The sediment traps were deployed using 4 metal pins (Fig. 6A) around the deployed ADVs at the same 5 locations (Fig. 1C). One trap is deployed in front of the ADV, one at the left side (looking seaward) and one at the right side (Fig. 6B). When removing the acrylic glass sediment traps from the surface, the bottom part was cleaned with a wipe. After analysing the results in the lab, it was noticed that the deposition at the mudflat was relatively low. This probably occurs due to a natural vegetation cover, which is situated at the bed around location MAB03 (Fig. 6C), the cover probably works as an armour layer, resulting in decreased levels of deposition. To collect more reasonable data, an extra sediment trap is located at the bed without the vegetation cover, close to the ADV at MAB03 (Fig. 6D). The acrylic glass sediment trap (0.20m x 0.20m) was chosen as the final design. The canvas sediment trap did not act as expected, due to bulging of the canvas. In addition filtering the deposited sediment was an extensive process due to the size of the trap. The acrylic glass trap of 0.20m x 0.20m is chosen, because the results are more reliable compared to the 0.15m x 0.15m trap and the time to process the deposited sediment still was reasonable.

Measurements were conducted at 24 March and 5 April 2015 at the locations MA01 (three traps), MA02 (three traps) and MAB03 (one trap) and at 25 March and 6 April 2015 at the locations MB01 (three traps), MB02 (three traps) and MAB03 (one trap).

**FIGURE 5. TESTING THE CANVAS SEDIMENT TRAP, FROM LEFT TO RIGHT: THE CANVAS TRAP DEPLOYED IN THE MANGROVE (A) AND THE BULGING EFFECT OF THE TRAP DURING HIGH TIDE (B).**
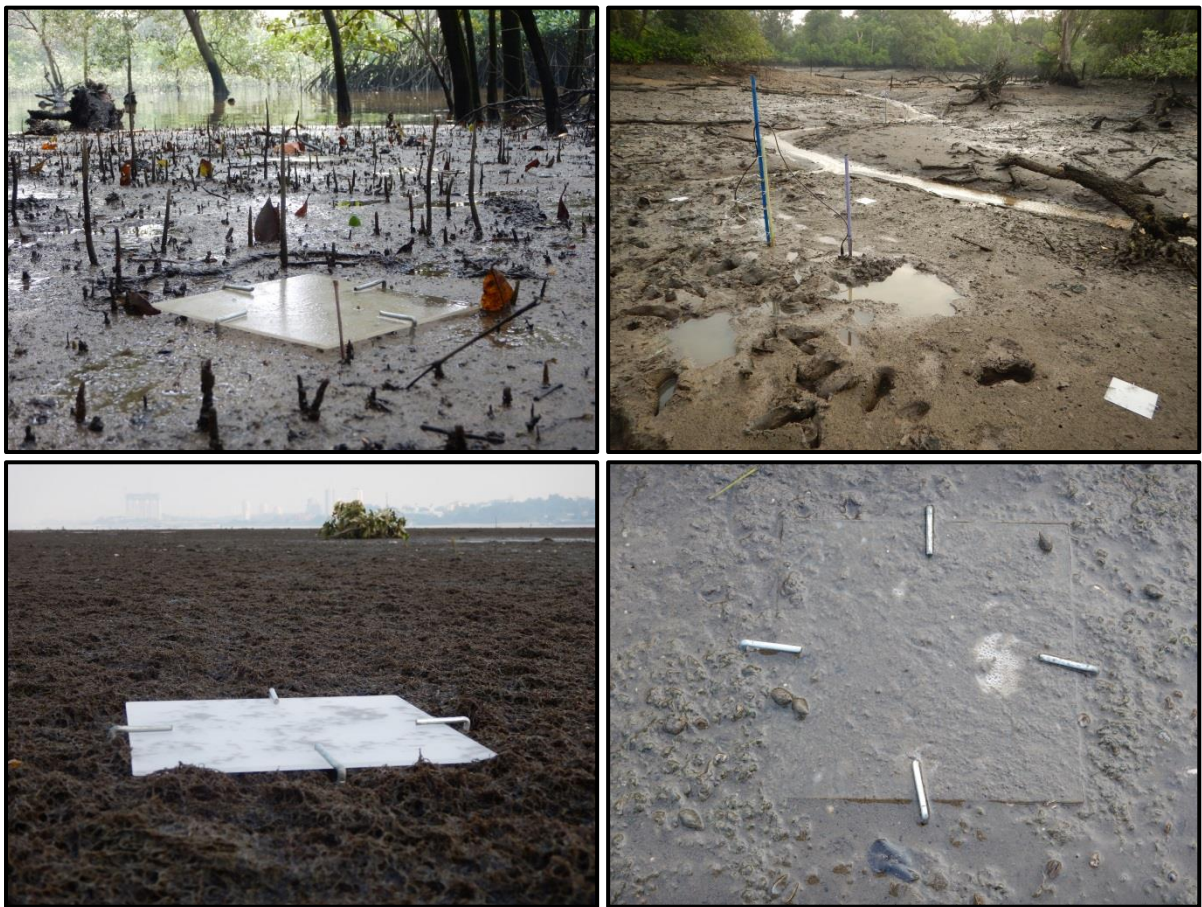


**FIGURE 6. DEPLOYMENT OF THE ACRYLIC GLASS SEDIMENT TRAPS, FROM TOP LEFT TO BOTTOM RIGHT: A SEDIMENT TRAP AT LOCATION MA01 (A), THREE SEDIMENT TRAPS AT LOCATION MA02 (B), A SEDIMENT TRAP IN THE VEGETATION COVER AT LOCATION MAB03 (C) AND A SEDIMENT TRAP AT LOCATION MAB03 AT THE MUDDY PART.**

## 2.3.   ACOUSTIC DOPPLER VELOCIMETERS.

Acoustic Doppler Velocimeters (ADVs) are used to collect water level data, flow velocity data, flow direction data and data regarding suspended sediment concentrations (SSC). Three ADVs are used with similar characteristics (table 3). The settings of the ADVs during the field measurements and for calibrating the SNR-SSC ratio (Section 2.3.3.1. Relation SNR – SSC) were different (table 4).

The ADV consists of a cylindrical probe and a head, the head can measure inter alia flow velocities, flow directions, signal to noise ratios (SNR), etc. Sensors present in the probe are: a pressure sensor, a temperature

sensor a tilt sensor and a compass. The latter two cannot be used as reference data for the head (where flow velocities and SSC values are measured), because the head is connected with the probe by a flexible cable.

The ADVs are deployed at the five locations shown in figure 1C. During a measurement period the three ADVs are deployed at the Mandai transect the first day and they are deployed at the locations MB01, MB02 and MAB03 during the second day. As mentioned before, location MAB03 (mudflat) is used for all measurement periods and can function as a reference location. The ADVs are deployed using bamboo canes, a clamp and tie wraps. The cylindrical probe is mounted with tie wraps at a bamboo cane that is driven in the soil. The probe is buried, so that the end bell is 7cm above the bed level. For mounting the head, one bamboo cane is driven into the soil and a second bamboo cane is mounted to the buried bamboo cane with tie wraps. The head is connected to the bamboo cane with a self-made clamp (Fig. 7). To create only minor disturbances, the clamp and bamboo canes were located perpendicular to the prevailing flow directions of the incoming and outgoing tide. The reference probe at the head of each ADV was aligned north. The head is mounted 23 cm above the bed, so that the measurement volume is 7 cm above the bed (Fig. 7), while the distance between the head and the vertical centre of the measurement volume is 16 cm (Fig. 7). A similar set-up is used before, only showing minor disturbances (Horstman et al. 2011; Horstman et al. 2013). The height of the measurement volume is 14 mm (Nortek 2005). The equipment is deployed before the measurement locations are exposed to high tide and the equipment is removed after high tide. The bamboo canes are left at the study site to guarantee the use of similar locations for consecutive measurements.

**TABLE 1. CHARACTERISTICS OF THE USED NORTEK ADVS.**

|  | 1 | 2 | 3 |
|---|---|---|---|
| Mark | Red | Blue | Grey |
| Instrument ID | VEC 9023 | VEC 3346 | VEC 9028 |
| Head ID | VEC 4775 | VEC 6500 | VEC 4759 |
| Number of beams | 3 | 3 | 3 |
| Firmware version | 3.33 | 1.21 | 3.33 |
| Software version | 1.29 | 1.29 | 1.29 |
| Recorder size [MB] | 361 | 82 | 361 |
| Head frequency [MHz] | 6 | 6 | 6 |

**TABLE 2. SETTINGS OF THE ADVS DURING CALIBRATING THE SNR – SSC RATIO AND DURING THE FIELD MEASUREMENTS.**

|  | Calibration | Field |
|---|---|---|
| Sampling rate [Hz] | 16 | 16 |
| Nominal velocity range [m/s] | 0.30 | 0.30 |
| Burst interval [s] | Continuous | 600 |
| Sampling volume [mm] | 14.9 | 14.9 |
| Transmit length [mm] | 4.0 | 4.0 |
| Receive length [m] | 0.01 | 0.01 |
| Velocity scaling [mm] | 0.1 | 0.1 |
| Power level [-] | Low+ | Low+ |
| Coordinate system [-] | XYZ | XYZ |
| Sound speed [-] | Measured | Measured |
| Salinity [ppt] | 11.0 | 11.0 |
| Distance between pings [-] | 1.01 | 1.01 |

**FIGURE 7. DEPLOYMENT OF THE ADVS, FROM TOP LEFT TO BOTTOM RIGHT: DIMENSIONS OF THE HEAD OF THE ADV, WITH THE MEASUREMENT VOLUME AS A BLUE DOT (A), DEPLOYED ADV AT THE *SONNERATIA* PATCH (B), DEPLOYED ADV AT THE BACK OF THE MANGROVE (C).**

### 2.3.1. WATER LEVELS

Water levels are indirectly measured at five locations (Fig. 3). The measurements are conducted with the pressure sensors located in the end bell of the ADV probe. The settings during fieldwork and calibration of the SNR-SSC relation (section 2.3.3.1. Relation SNR-SSC) were slightly different (table 4). The range of the pressure sensors is 0 – 20m with an accuracy of 0.25% of the full scale and a resolution of 0.005% of the full scale (Nortek 2005). The resulting data is pre-processed using filtering, averaging and data correction, similar to Horstman et al. (2013). Inaccurate data is removed by only selecting data above a mean correlation threshold for the return signals of the ADV's receiver probes, which is 80% (SonTek 1997; Chanson et al. 2008). Due to the filtering procedure major disturbances (e.g. shipping or animal activity) and minor disturbances (e.g. air bubbles) were removed. After filtering the data was burst averaged (1 burst is equal to 600 s) to remove

fluctuations caused by wind and swell waves. The filtered data showed continuous data without gaps during high tide.

The probe is buried in the soil, with the end bell and its pressure sensor 7 cm above the bed level, equal to the deployment settings of Horstman (2013). When comparing the results from the different pressure sensors, it seemed that they were not accurate. The sensors are calibrated by putting the ADVs in transparent tubes with measuring tape mounted on the outside (Fig. 8B). ADV 1 and 3 (Red and Grey) are calibrated together by releasing water from the transparent tube and ADV 2 (Blue) is calibrated by filling up a smaller transparent tube (Fig. 8E). The measurements are done by measuring a certain water level for a minute followed by a water level adaptation of 5 cm (Fig. 9). ADV 2 (Blue) has the most accurate pressure sensor, despite the constant couple of centimetres offset. The measured water levels by ADV 2 (Blue), in combination with measured bed level differences between the measurement locations, can be used to extrapolate water levels to all locations. It is assumed that a water level gradient is not present in Mandai mangrove, due to the small extent. Elevation data is collected for correcting the water levels at the other locations, using ADV 2. The data is collected with the Nikon Forestry Pro Laser Rangefinder in combination with a measurement pole. The pole was located at the arrowheads, while the Nikon Forestry Pro was located at the base of the arrow at a fixed height (Fig. 10 & 11 and table 5 & 6). The raw data (Fig. 10 & 11 and table 5 & 6) is converted to bed level differences between the different measurement locations with measurement locations MAB03 (mudflat) and MA02 (*Sonneratia* patch), both with similar bed levels, as reference (Fig. 12).



FIGURE 8. CALIBRATING THE PRESSURE SENSORS, FROM TOP LEFT TO BOTTOM RIGHT: MOUNTING ADV 1 (RED) AND ADV 3 (GREY) TOGETHER (A), MEASURING THE PRESSURE OF ADV 1 AND 3 AT A WATER LEVEL OF 0.7M (B), THE SET UP FOR MEASURING ADV 2 (BLUE) (D) AND MEASURING THE PRESSURE OF ADV 2 (BLUE) (E).
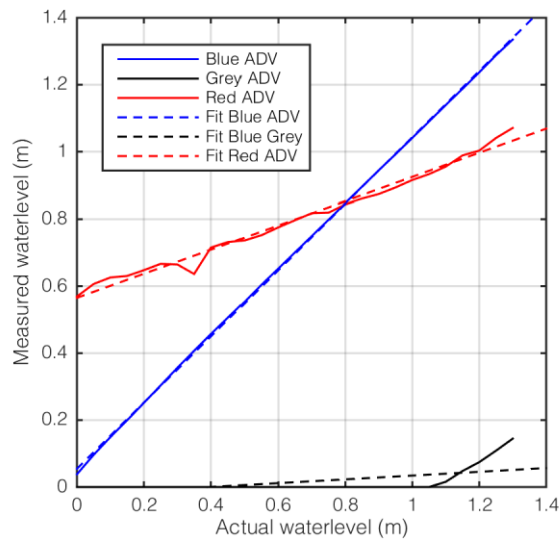
**FIGURE 9. THE ACTUAL WATER LEVEL RELATED TO THE MEASURED WATER LEVEL**
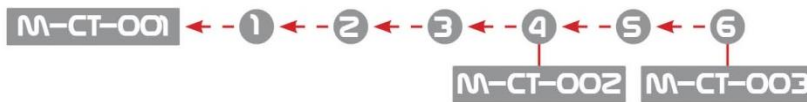


**FIGURE 10. MEASUREMENT LOCATIONS AND STEPS AT THE MANDAI TRANSECT.**

**TABLE 3. COLLECTED DATA AT THE MANDAI TRANSECT (MA01, MA02, MAB03).**

| Measurement [#] | Angle [deg.] | Distance [m] | Angle [rad.] | Elevation dist. [m] |
|---|---|---|---|---|
| 1 | -1.4 | 37.4 | -0.0244 | -0.9140 |
| 2 | 0.0 | 41.0 | 0.0000 | 0.0000 |
| 3 | -1.2 | 41.8 | -0.0209 | -0.8756 |
| 4 | -0.6 | 33.4 | -0.0105 | -0.3498 |
| 5 | -0.3 | 21.4 | -0.0052 | -0.1121 |
| 6 | 0.8 | 32.0 | 0.0140 | 0.4468 |
| 7 | 1.4 | 22.4 | 0.0244 | 0.5474 |
| 8 | 1.2 | 27.4 | 0.0209 | 0.5739 |
| 9 | 0.6 | 32.4 | 0.0105 | 0.3393 |
| 10 | 3.0 | 11.0 | 0.0524 | 0.5765 |
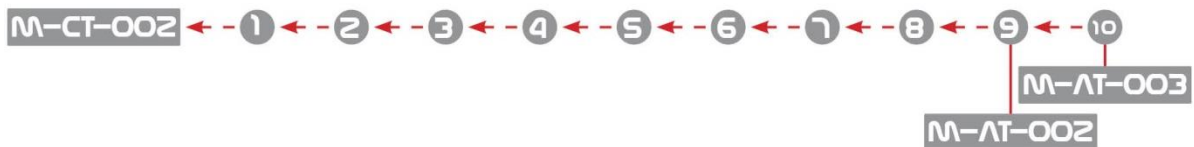


**FIGURE 11. MEASUREMENT LOCATIONS AND STEPS PERPENDICULAR TO THE MANDAI TRANSECT.**

**TABLE 4. COLLECTED DATA PERPENDICULAR TO THE MANDAI TRANSECT (MB01, MB02, MAB03).**

| Measurment [#] | Angle [deg.] | Distance [m] | Angle [rad.] | Elevation dist. [m] |
|---|---|---|---|---|
| 1 | 1.4 | 23.0 | 0.0244 | 0.5621 |
| 2 | 0.8 | 26.4 | 0.0140 | 0.3686 |
| 3 | 0.4 | 28.0 | 0.0070 | 0.1955 |
| 4 | 0.0 | 22.8 | 0.0000 | 0.0000 |
| 5 | 0.0 | 37.0 | 0.0000 | 0.0000 |
| 6 | 0.0 | 62.0 | 0.0000 | 0.0000 |
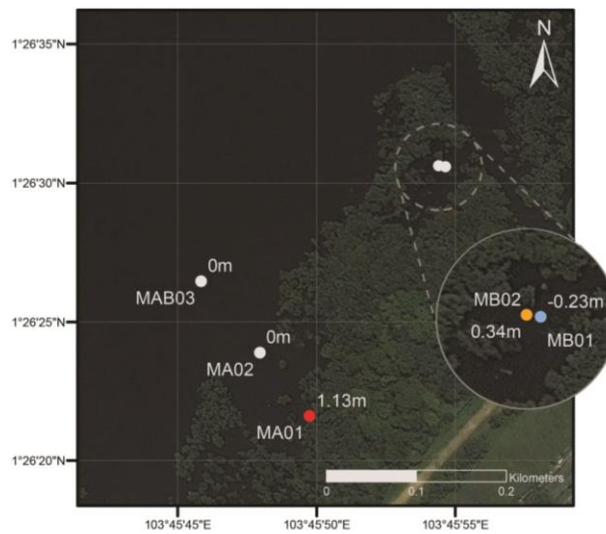
**FIGURE 12. ELEVATION DIFFERENCES BETWEEN MEASUREMENT LOCATIONS**

### 2.3.2. FLOW VELOCITY

Flow velocities and flow directions are measured at all five locations (Fig. 3) with three ADVs, using the XYZ setting for the coordinate system of the ADVs (Table 3 & 4). The resulting data is pre-processed similar to pre-processing the water level data. The horizontal flow velocities are obtained using Matlab scripts.

### 2.3.3. SUSPENDED SEDIMENT CONCENTRATIONS

Suspended sediment concentrations (SSCs) are collected indirectly by deploying ADVs at all five locations (Fig. 3) and measuring the signal to noise ratio (SNR). The settings of the ADVs were different from the settings during the calibration (table 3 & 4). The resulting data is pre-processed similar to pre-processing the water level data. Matlab scripts are used to convert the SNR to SSC using the calibration relation showed in the next section.

#### 2.3.3.1. RELATION SNR – SSC

The suspended sediment concentration (SSC) can be calculated with the SNR, an output from the ADVs. The ADV is deployed in a bucket of tap water, with a volume of 12 L, (Fig. 13A) and salt is added until a concentration of 11 ppt is reached, which is kept constant during the calibration. Wet mud is added in consecutive steps (estimated with the results in Horstman (2013)) (table 7). The solution is kept into motion with a stick and after adding wet mud a measurement is done for 3 minutes. When the measurement is finished, a sample of 50 ml is collected at the height of the measurement volume, as close as possible to the measurement volume (Fig. 13B). After collecting 14 samples, the samples are filtered (Fig. 13C) and the pre-weighted filters are collected (Fig. 13D). The filters are oven-dried at 105⁰C for 24 hours (Fig. 13e) and weighted again (table 7).

The resulting relation between the SNR and SSC (Fig. 14) is showed in the equation below, with an $R^2$ value of 0.92:

$$\log(SSC) = 0.1773 * SNR - 4.3396$$

The resulting curve (Fig. 15) is comparable with SSC – SNR correlations in Salehi et al. (2011). Calibration curves from Voulgaris et al. (2004), Chanson et al. (2008), Ha et al. (2009), Horstman et al. (2013) show a slightly lower curve, resulting in smaller SSC values for similar SNR values. However the gradient of the calibration curve from this study is similar to the relation showed by Voulgaris et al. (2004), Salehi et al. (2011) and Horstman et al. (2013). Relations showed by Chanson et al. (2008) and Ha et al. (2009) show relations with a remarkable gradient (almost horizontal lines (Fig. 15)).
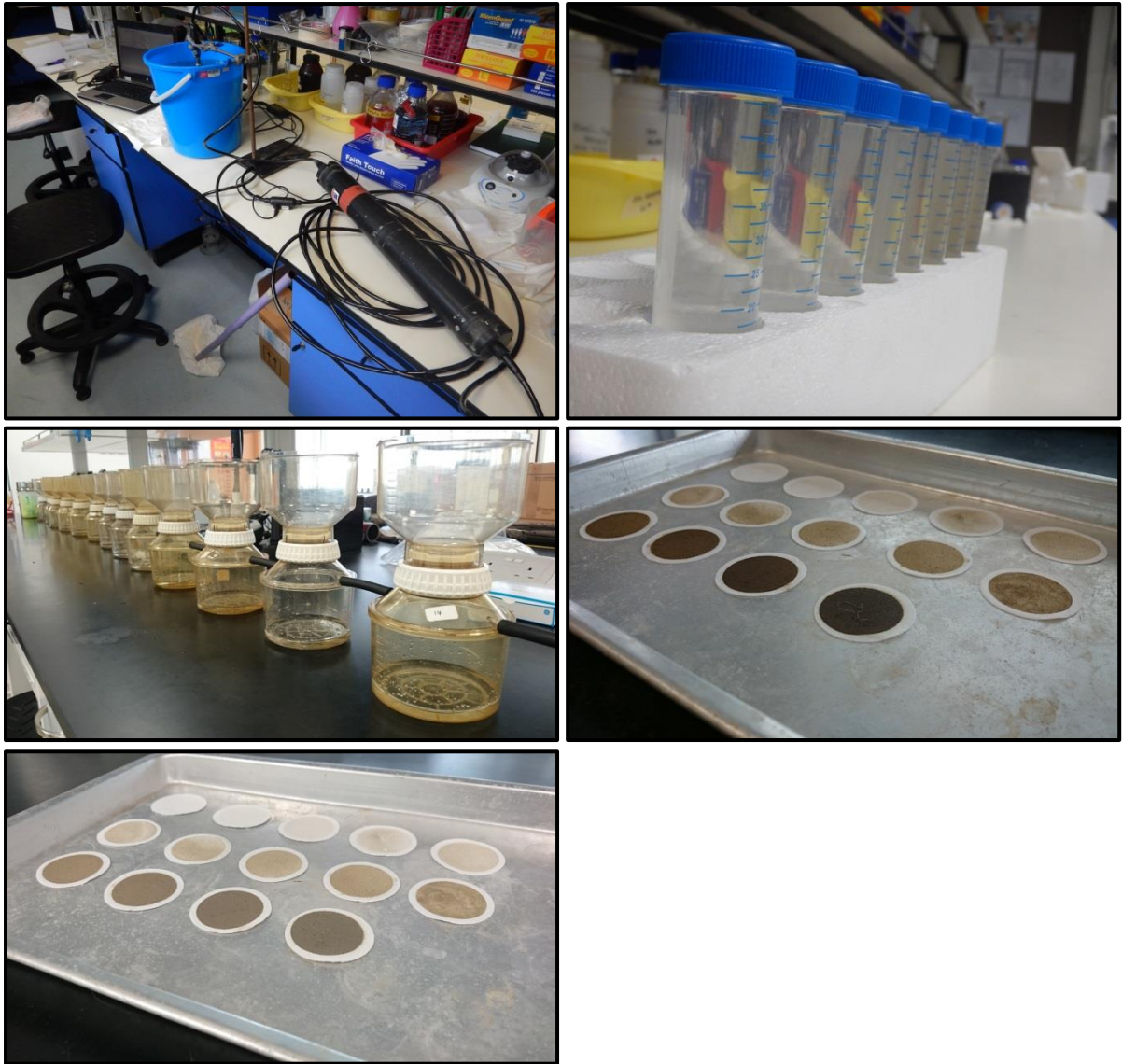
**FIGURE 13. CALIBRATING THE SNR TO SSC RELATION, FROM TOP LEFT TO BOTTOM RIGHT: LAB SET UP (A), SSC SAMPLES (B), FILTRATION SET UP (C), FILTERS BEFORE OVEN-DRYING (D), FILTERS AFTER OVEN-DRYING (E).**

**TABLE 5. DATA COLLECTED DURING CALIBRATING THE SNR - SSC RELATION.**

| Estimated SSC [mg l$^{-1}$] | Estimated wet mud added total [g] | Estimated wet mud added per step [g] | Wet mud added total [g] | Wet mud added per step [g] | Sample [#] | Filename | Start time [h:mm:ss] | End time [h:mm:ss] | Average SNR beam 1 | SD SNR beam 1 | Average SNR beam 2 | SD SNR beam 2 | Average SNR beam 3 | SD SNR beam 3 | SNR Total Average | Mass dry filter [g] | Mass dry sediment and filter [g] | Mass dry sediment [g] | SSC [mg l$^{-1}$] |
|---|---|---|---|---|---|---|---|---|---|---|---|---|---|---|---|---|---|---|---|
| 10 | 0.40 | 0.40 | 0.39 | 0.39 | 1 | SSC1 | 2:49:08 | 2:52:18 | 31.36 | 1.07 | 37.51 | 1.21 | 33.03 | 1.12 | 33.97 | 0.1295 | 0.1318 | 0.0023 | 46 |
| 25 | 0.99 | 0.60 | 1.00 | 0.61 | 2 | SSC2 | 3:06:04 | 3:09:19 | 31.76 | 1.08 | 37.48 | 1.29 | 33.03 | 1.13 | 34.09 | 0.1298 | 0.1317 | 0.0019 | 38 |
| 50 | 1.98 | 0.99 | 2.39 | 1.39 | 3 | SSC3 | 3:18:10 | 3:21:19 | 32.27 | 1.15 | 37.97 | 1.35 | 33.43 | 1.30 | 34.55 | 0.1283 | 0.1310 | 0.0027 | 54 |
| 100 | 3.97 | 1.98 | 4.01 | 1.62 | 4 | SSC4 | 3:38:33 | 3:41:39 | 33.20 | 1.34 | 38.89 | 1.40 | 34.88 | 1.37 | 35.66 | 0.1292 | 0.1325 | 0.0033 | 66 |
| 150 | 5.95 | 1.98 | 6.05 | 2.04 | 5 | SSC5 | 3:48:17 | 3:51:19 | 32.82 | 1.41 | 38.93 | 1.48 | 35.02 | 1.50 | 35.59 | 0.1293 | 0.1338 | 0.0045 | 90 |
| 200 | 7.94 | 1.98 | 8.06 | 2.01 | 6 | SSC6 | 3:57:47 | 4:01:01 | 33.81 | 1.40 | 39.26 | 1.39 | 35.19 | 1.50 | 36.09 | 0.1294 | 0.1342 | 0.0048 | 96 |
| 250 | 9.92 | 1.98 | 10.00 | 1.94 | 7 | SSC7 | 4:10:21 | 4:13:31 | 32.34 | 1.20 | 38.33 | 1.26 | 34.67 | 1.20 | 35.11 | 0.1281 | 0.1338 | 0.0057 | 114 |
| 300 | 11.91 | 1.98 | 11.95 | 1.95 | 8 | SSC8 | 4:18:51 | 4:21:54 | 33.56 | 1.57 | 39.57 | 1.50 | 36.02 | 1.51 | 36.38 | 0.1280 | 0.1345 | 0.0065 | 130 |
| 400 | 15.88 | 3.97 | 15.91 | 3.96 | 9 | SSC9 | 4:27:36 | 4:30:41 | 34.95 | 1.83 | 39.32 | 1.73 | 34.68 | 1.64 | 36.32 | 0.1295 | 0.1375 | 0.0080 | 160 |
| 500 | 19.85 | 3.97 | 19.86 | 3.95 | 10 | SSC10 | 4:42:12 | 4:54:17 | 33.76 | 1.37 | 39.57 | 1.43 | 34.87 | 1.38 | 36.07 | 0.1282 | 0.1376 | 0.0094 | 188 |
| 750 | 29.77 | 9.92 | 29.79 | 9.93 | 11 | SSC11 | 4:52:13 | 4:55:18 | 35.51 | 1.86 | 41.26 | 1.65 | 36.72 | 1.77 | 37.83 | 0.1292 | 0.1410 | 0.0118 | 236 |
| 1000 | 39.70 | 9.92 | 39.67 | 9.88 | 12 | SSC12 | 5:02:13 | 5:05:18 | 36.38 | 1.71 | 41.60 | 1.50 | 37.18 | 1.66 | 38.38 | 0.1285 | 0.1439 | 0.0154 | 308 |
| 1500 | 59.54 | 19.85 | 59.52 | 19.85 | 13 | SSC13 | 5:10:07 | 5:13:12 | 37.27 | 1.71 | 42.47 | 1.50 | 38.27 | 1.71 | 39.33 | 0.1278 | 0.1498 | 0.0220 | 440 |
| 2000 | 79.39 | 19.85 | 79.38 | 19.86 | 14 | SSC14 | 5:18:48 | 5:21:58 | 38.51 | -1.69 | 43.92 | -1.36 | 39.68 | -1.63 | 40.70 | 0.1290 | 0.1599 | 0.0309 | 618 |
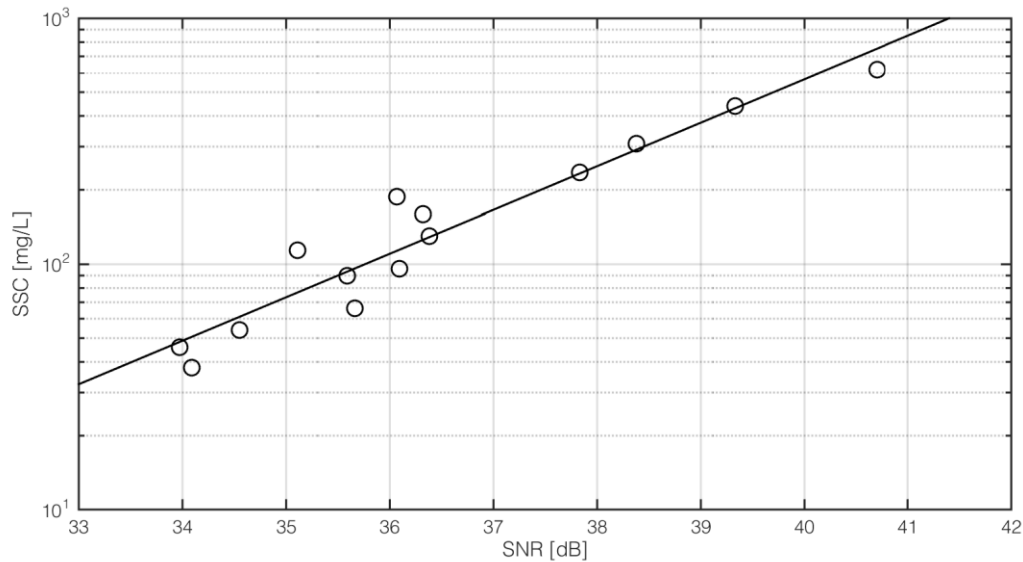


FIGURE 14. SSC - SNR CURVE AFTER CALIBRATION, WITH A FITTED (BLACK CONTINUOUS) LINE, THROUGH THE MEASURED SAMPLES (POINTS). THE RESULTING R$^2$ IS 0.92.

**TABLE 6: CHARACTERISTICS FOR CALIBRATING THE SNR – SSC RELATION FOR ADVS IN OTHER STUDIES.**

| Author(s) | Equipment | Power level | Head freq. [MHz] | Vel. Range [m s$^{-1}$] | $d_{50}$ [μm] | $d_m$ [μm] | Relation | $R^2$ |
|---|---|---|---|---|---|---|---|---|
| Horstman et al. (2013) | Nortek Vector | Low | 6 | 0.3 | 66.5 | | log(SSC)=0.1849*SNR-5.892 | 0.94 |
| Salehi et al. (2011) | Nortek Vector | Low | 6 | 1-2 | 5.2 | 7.9 | log(SSC)=0.099*SNR-1.253 | 0.99 |
| Salehi et al. (2011) | Nortek Vector | Low | 6 | 1-2 | 5.4 | 8.3 | log(SSC)=0.103*SNR-1.677 | 1 |
| Salehi et al. (2011) | Nortek Vector | Low | 6 | 1-2 | 20.9 | 46 | log(SSC)=0.171*SNR-5.670 | 0.98 |
| Chanson et al. (2008) | Sontek 2D MicroADV | - | 16 | 0.1 | - | - | log(SSC)=log(0.9426*(1-exp(-0.1109*SNR))) | 0.99 |
| Ha et al. (2009) | Sontek ADVOcean | - | 5 | 5 | 1 | - | log(SSC)=0.172*SNR-9.983 | 0.91 |
| Ha et al. (2009) | Sontek ADVOcean | - | 5 | 5 | 88 | - | log(SSC)=0.019*SNR-1.407 | 0.96 |
| Voulgaris et al. (2004) | Sontek ADV | - | 10 | - | - | - | log(SSC)=10.8*log(SNR)-17.8 | ? |
| This study | Nortek Vector | Low | 6 | 0.3 | 27.3 - 649 | - | log(SSC)=0.1773*SNR-4.3396 | 0.92 |
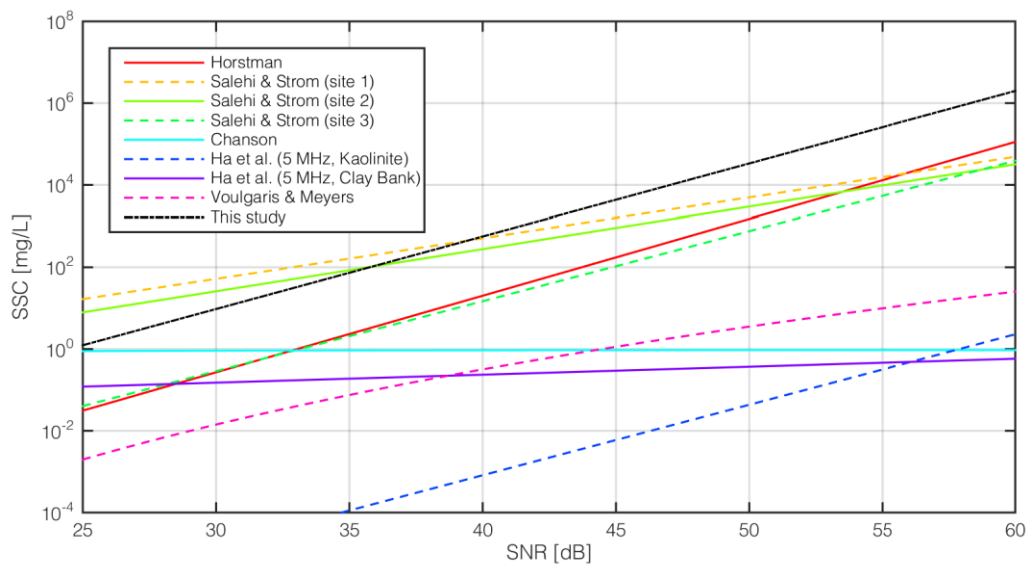


FIGURE 15. COMPARISON BETWEEN SNR - SSC CALIBRATION CURVES FROM THIS STUDY WITH STUDIES FROM VOULGARIS ET AL. (2004), CHANSON ET AL. (2008), HA ET AL. (2009), SALEHI ET AL. (2011) AND HORSTMAN ET AL. (2013).

### 2.3.4. PROFILE MEASUREMENTS

The ADVs only collect point data at the specific vertical level of deployment. By deploying ADVs at a vertical profile, data can be collected over a water column. To get insights in the vertical velocity profiles and SSC profiles, the three ADVs are deployed at the same location at 7 April 2015. The ADVs are located in the tidal creek, MB01 (Fig. 1C). The measurement volumes from the different ADVs are located at: 7 cm (Grey ADV), 22 cm (Blue ADV) and 92 cm (Red ADV) from the bed level (Fig. 16).
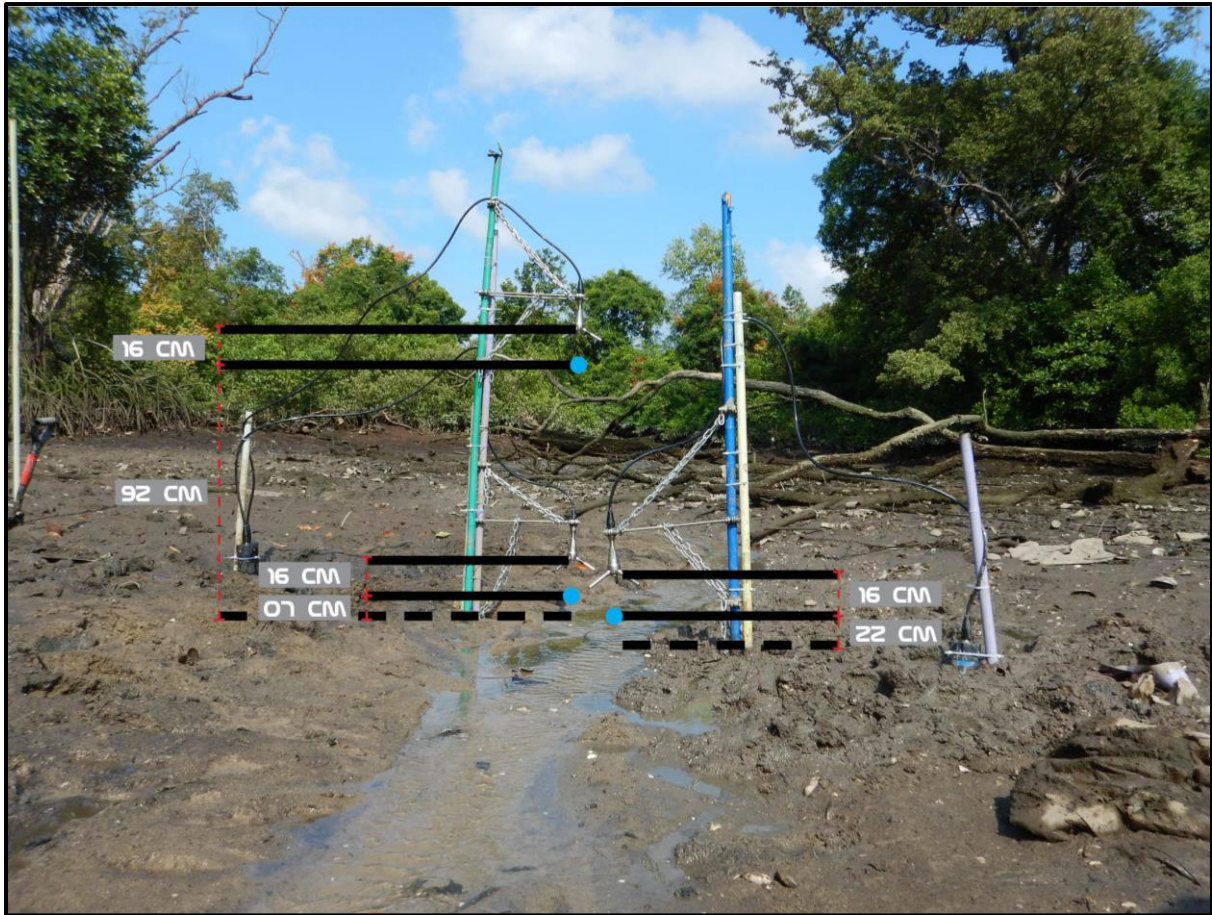
**FIGURE 16. ADVS DEPLOYED TO MEASURE FLOW VELOCITIES AND SSC PROFILES, WITH THE MEASUREMENT VOLUMES SHOWED BY THE BLUE DOTS.**

## 2.4.    SEDIMENT CHARACTERISTICS

Soil samples are collected at all measurement locations (including the extra measurement location at the mudflat), resulting in samples from six different locations. The samples represent the top layer (<2cm) of the soil. Sediment samples at these locations are taken at 22 March 2015 and at 06 April 2015. The grain size characteristics from the extra measurement location at the mudflat is used as the representative grain size distribution, due to a cover of vegetation at the location where the ADV is situated. The samples are analysed at the NIOZ located in Yerseke, the Netherlands (according to their standards). In addition to conducting a particle size analysis, the organic matter content is analysed.

# 3. COLLECTED DATA

The collected data regarding: sediment deposition, grain size characteristics, organic matter content, suspended sediment concentrations (SSCs), water levels, flow velocities and vegetation characteristics, is presented in this section. The measurements were executed during two periods: 24-25 March 2015 and 5-7 April 2015.

## 3.1. VEGETATION

Vegetation is measured according to the methods described in the previous section (2.1. Vegetation), resulting in 56 sampled *Sonneratia* saplings (table 7) and five representative *Sonneratia* trees (table 8), representing two patches (Fig. 1D) of trees (table 9).

**TABLE 7. DIMENSIONS OF SAMPLED *SONNERATIA* SAPLINGS.**

| # [-] | Circumf. bottom [cm] | Diam. bottom [cm] | Largest Diam. incl. branches [cm] | Height [cm] | Height first split [cm] | Circumf. trunks above split [cm] | | | |
|---|---|---|---|---|---|---|---|---|---|
| 1 | 14.20 | 4.52 | 100.00 | 161.00 | 55.00 | 16.90 | 20.00 | | |
| 2 | 15.00 | 4.77 | 90.00 | 147.00 | 33.00 | 14.00 | 14.00 | | |
| 3 | 10.00 | 3.18 | 86.00 | 97.00 | 8.00 | 10.00 | <5 | | |
| 4 | 7.80 | 2.48 | 78.00 | 97.00 | 0.00 | 7.80 | 6.80 | | |
| 5 | 17.00 | 5.41 | 90.00 | 175.00 | 15.00 | 10.00 | 16.00 | | |
| 6 | 12.90 | 4.11 | 83.00 | 147.00 | 0.00 | 12.90 | 9.00 | | |
| 7 | 12.00 | 3.82 | 190.00 | 109.00 | 0.00 | 12.00 | 7.20 | 6.00 | |
| 8 | 11.00 | 3.50 | 138.00 | 106.00 | 0.00 | 10.00 | 11.00 | | |
| 9 | 18.20 | 5.79 | 58.00 | 95.00 | 0.00 | 18.20 | 11.00 | | |
| 10 | 20.70 | 6.59 | 126.00 | 184.00 | 0.00 | 20.70 | 7.50 | | |
| 11 | 9.00 | 2.86 | 86.00 | 113.00 | 0.00 | 9.00 | 6.10 | | |
| 12 | 14.00 | 4.46. | 134.00 | 83.00 | 0.00 | 7.00 | 11.00 | | |
| 13 | 12.00 | 3.82 | 180.00 | 119.00 | 0.00 | 12.00 | 10.00 | | |
| 14 | 16.80 | 5.35 | 150.00 | 190.00 | 43.00 | 11.00 | 13.30 | | |
| 15 | 13.00 | 4.14 | 80.00 | 140.00 | 0.00 | 13.00 | 10.00 | | |
| 16 | 16.00 | 5.09 | 140.00 | 173.00 | 0.00 | 16.00 | <5 | <5 | |
| 17 | 18.00 | 5.73 | 123.00 | 184.00 | 49.00 | 12.00 | 11.50 | | |
| 18 | 17.00 | 5.41 | 150.00 | 140.00 | 0.00 | 17.00 | 9.50 | | |
| 19 | 10.00 | 3.18 | 72.00 | 60.00 | 14.00 | 8.00 | <5 | | |
| 20 | 8.00 | 2.55 | 83.00 | 77.00 | | | | | |
| 21 | 8.20 | 2.61 | 57.00 | 90.00 | | | | | |
| 22 | 9.00 | 2.86 | 100.00 | 77.00 | | | | | |
| 23 | 18.90 | 6.02 | 115.00 | 127.00 | 0.00 | 18.90 | 12.00 | | |
| 24 | 7.20 | 2.29 | 64.00 | 80.00 | | | | | |
| 25 | 7.30 | 2.32 | 78.00 | 96.00 | 0.00 | 7.30 | <5 | <5 | <5 | <5 |
| 26 | 12.70 | 4.04 | 140.00 | 135.00 | 1.00 | 12.70 | 11.00 | | |
| 27 | 11.00 | 3.50 | 81.00 | 95.00 | | | | | |
| 28 | 10.00 | 3.18 | 40.00 | 94.00 | | | | | |
| 29 | 10.00 | 3.18 | 130.00 | 61.00 | 0.00 | 9.00 | 10.00 | | |
| 30 | 16.00 | 5.09 | 195.00 | 195.00 | | | | | |
| 31 | 6.80 | 2.16 | 73.00 | 73.00 | 1.00 | <5 | | | |
| 32 | 13.00 | 4.14 | 170.00 | 158.00 | 57.00 | 12.00 | <5 | | |
| 33 | 12.20 | 3.88 | 102.00 | 182.00 | | | | | |
| 34 | 6.80 | 2.16 | 87.00 | 97.00 | 0.00 | 6.80 | 3.00 | | |
| 35 | 9.00 | 2.86 | 80.00 | 99.00 | 0.00 | 9.00 | 5.00 | | |
| 36 | 9.00 | 2.86 | 50.00 | 95.00 | | | | | |
| 37 | 7.30 | 2.32 | 62.00 | 92.00 | | | | | |
| 38 | 11.00 | 3.50 | 97.00 | 78.00 | | | | | |
| 39 | 9.00 | 2.86 | 134.00 | 70.00 | 0.00 | 9.00 | 5.90 | <5 | |
| 40 | 12.00 | 3.82 | 82.00 | 110.00 | 20.00 | 10.00 | 9.50 | | |
| 41 | 9.60 | 3.06 | 45.00 | 95.00 | 50.00 | <5 | <5 | | |

| # | | | | | | | |
|---|---|---|---|---|---|---|---|
| 42 | 13.00 | 4.14 | 99.00 | 140.00 | 0.00 | 13.00 | 10.00 |
| 43 | 15.90 | 5.06 | 140.00 | 103.00 | 15.00 | 12.30 | 11.40 |
| 44 | 10.00 | 3.18 | 90.00 | 150.00 | 47.00 | 10.00 | 8.00 |
| 45 | 6.80 | 2.16 | 95.00 | 85.00 | 0.00 | 6.80 | <5 |
| 46 | 10.00 | 3.18 | 79.00 | 67.00 | | | |
| 47 | 7.00 | 2.23 | 52.00 | 90.00 | 16.00 | 7.20 | <5 |
| 48 | 7.00 | 2.23 | 63.00 | 80.00 | 1.00 | <5 | <5 |
| 49 | 8.00 | 2.55 | 108.00 | 77.00 | 20.00 | <5 | <5 |
| 50 | 8.70 | 2.77 | 95.00 | 100.00 | 0.00 | 8.70 | 6.50 | <5 |
| 51 | 17.30 | 5.51 | 101.00 | 165.00 | 0.00 | 17.30 | 7.20 |
| 52 | 7.00 | 2.23 | 61.00 | 90.00 | 38.00 | <5 | <5 |
| 53 | 8.00 | 2.55 | 80.00 | 68.00 | 0.00 | 8.00 | <5 |
| 54 | 7.00 | 2.23 | 45.00 | 81.00 | 47.00 | <5 | <5 |
| 55 | 4.20 | 1.34 | 35.00 | 90.00 | 0.00 | 0.00 | |
| 56 | 10.00 | 3.18 | 115.00 | 89.00 | 3.00 | 9.80 | 10.00 |

**TABLE 8. DIMENSIONS OF THE SAMPLED *SONNERATIA* TREES.**

| # [-] | Circumf. [cm] | DBH [cm] | Circumf. bottom [cm] | Diam. bottom [cm] | Largest Diam. below DBH [cm] |
|---|---|---|---|---|---|
| 1 | 16.00 | 5.09 | 25.80 | 8.21 | 164.00 |
| 2 | 7.20 | 2.29 | 13.20 | 4.20 | 80.00 |
| 3 | 10.80 | 3.44 | 19.20 | 6.11 | 100.00 |
| 4 | 12.00 | 3.82 | 23.00 | 7.32 | 126.00 |
| 5 | 14.80 | 4.71 | 14.00 | 4.46 | 90.00 |

**TABLE 9. NUMBER OF *SONNERATIA* TREES IN THE MEASURED PATCHES (FIG. 1D).**

| Location | Number of trees (#) |
|---|---|
| Northern patch | 25 |
| Southern patch | 23 |

## 3.2.    ADV DATA

A summary, including a quality check, shows the resulting datasets (table 10). After deploying the ADVs, in a test period, not all ADVs were measuring correctly, due to some electronical issues. These issues were solved before deploying the ADVs for the real measurements. Problems with the pressure sensors still occurred, as mentioned previously (2.3.1. Water levels). During the second period of measurements (05 – 07 April 2015), measured correlations were remarkable low, resulting in data that cannot be used. Graphs of the first measurement period (24 – 25 March 2015) are showed in the next subsections.

**TABLE 10. SUMMARY OF THE DATA COLLECTED WITH THE ADVS.**

| Location | Date | ADV | Measurement | Data files |
|---|---|---|---|---|
| MA01 | 21-03-15 | Blue | Mudflat (test) | Man_0101 (Blue) |
| MA02 | 21-03-15 | Red | *Sonneratia* patch (test) | Man_0201 (Red) |
| MAB03 | 21-03-15 | Grey | Mudflat (test) | - |
| MB02 | 22-03-15 | Red | Tidal creekbank (test) | Man_0201 (Red) |
| MB01 | 22-03-15 | Blue | Tidal creek (test) | Man_0101 (Blue) |
| MAB03 | 22-03-15 | Grey | Mudflat (test) | - |
| MA01 | 24-03-15 | Grey | Mudflat | M_P2_101 (Grey) |
| MA02 | 24-03-15 | Blue | *Sonneratia* patch | M_P2_201 (Blue) |
| MAB03 | 24-03-15 | Red | Mudflat | M_P2_301 (Red) |
| MB02 | 25-03-15 | Blue | Tidal creekbank | M_P2_201 (Blue) |
| MB01 | 25-03-15 | Grey | Tidal creek | M_P2_101 (Grey) |
| MAB03 | 25-03-15 | Red | Mudflat | M_P2_301 (Red) |
| MA01 | 05-04-15 | Grey | Mudflat | M_P3_101 (Grey) |
| MA02 | 05-04-15 | Blue | *Sonneratia* patch | M_P3_201 (Blue) |
| MAB03 | 05-04-15 | Red | Mudflat | M_P3_301 (Red) |
| MB02 | 06-04-15 | Blue | Tidal creekbank | M_P3_201 (Blue) |
| MB01 | 06-04-15 | Grey | Tidal creek | M_P3_101 (Grey) |
| MAB03 | 06-04-15 | Red | Mudflat | M_P3_301 (Red) |
| MB01 | 07-04-15 | Grey | Flow velocity | M_P3_101 (Grey) |
| MB01 | 07-04-15 | Red | Flow velocity | M_P3_201 (Blue) |
| MB01 | 07-04-15 | Blue | Flow velocity | M_P3_301 (Red) |

| Location | Matlab file | Correlation around high tide [%] | SSC range around high tide [mg/L] | Flow velocity range around high tide [m/s] |
|---|---|---|---|---|
| MA01 | Plotting_ADV_measurements_Man_0101_21_03 | 98 | 0.1 - 0.5 | -0.01 - 0.01 |
| MA02 | Plotting_ADV_measurements_Man_0201_21_03 | 99 | 0.02 - 0.026 | -0.06 - 0.06 |
| MAB03 | - | - | - | - |
| MB02 | Plotting_ADV_measurements_Man_0201_22_03 | 20 | | -0.2 - 0.06 |
| MB01 | Plotting_ADV_measurements_Man_0101_22_03 | 99 | 0 - 15000 | -0.025 - -0.05 |
| MAB03 | - | - | - | - |
| MA01 | Plotting_ADV_measurements_M_P2_101_24_03 | 90 | 0 - 0.06 | -0.025 - 0.005 |
| MA02 | Plotting_ADV_measurements_M_P2_201_24_03 | 99 | 0 - 12 | -0.06 - 0.06 |
| MAB03 | Plotting_ADV_measurements_M_P2_301_24_03 | 99 | 0 - 2.7 | -0.06 - 0.06 |
| MB02 | Plotting_ADV_measurements_M_P2_201_25_03 | 85 | 0 - 0.014 | -0.03 - 0.04 |
| MB01 | Plotting_ADV_measurements_M_P2_101_25_03 | 95 | 0 - 0.07 | -0.06 - 0.06 |
| MAB03 | Plotting_ADV_measurements_M_P2_301_25_03 | 99 | 0 - 12 | -0.02 - 0.05 |
| MA01 | Plotting_ADV_measurements_M_P3_101_05_04 | 20 | 0 - 0.00015 | -0.1 - 0.05 |
| MA02 | Plotting_ADV_measurements_M_P3_201_05_04 | 99 | 0 - 0.7 | -0.06 - 0.06 |
| MAB03 | Plotting_ADV_measurements_M_P3_301_05_04 | 20 | 0 - 0.0045 | -0.2 - 0.05 |
| MB02 | Plotting_ADV_measurements_M_P3_201_06_04 | 95 | 0 - 1.6 | -0.03 - 0.05 |
| MB01 | Plotting_ADV_measurements_M_P3_101_06_04 | 98 | 0.05 - 0.4 | -0.08 - 0.06 |
| MAB03 | Plotting_ADV_measurements_M_P3_301_06_04 | 99 | 0 - 0.8 | -0.08 - 0.06 |
| MB01 | Plotting_ADV_measurements_M_P3_101_07_04 | 90 | 0 - 35 | -0.08 - 0.08 |
| MB01 | Plotting_ADV_measurements_M_P3_201_07_04 | 95 | 0 - 0.2 | -0.08 - 0.08 |
| MB01 | Plotting_ADV_measurements_M_P3_301_07_04 | 85 | 0 - 0.07 | -0.06 - 0.1 |

| Location | Main flow directions [deg.] | Max Water level [m] | Data quality |
|---|---|---|---|
| MA01 | 30 - 195 - 320 | 1.3 | Good. |
| MA02 | 45 - 240 | 0.6 | Good. Except pressure sensor (water levels). |
| MAB03 | - | - | No data at all. |
| MB02 | 45 - 250 | 0.7 | Bad. Correlation too low, data cannot be used. |
| MB01 | 240 | 0.4 | Bad. Only 60 minutes of data, data cannot be used. |
| MAB03 | - | - | No data at all. |
| MA01 | 255 - 315 | 0.07 | Good. Except pressure sensor (water levels). |
| MA02 | 45 - 240 | 1.7 | Good. |
| MAB03 | 45 - 195 | 0.5 | Good. Except pressure sensor (water levels). |
| MB02 | 105 - 315 | 1.6 | Good. |
| MB01 | 120 - 280 | 0.4 | Good. Except pressure sensor (water levels). |
| MAB03 | 170 - 300 | 0.6 | Good. Except pressure sensor (water levels). |
| MA01 | 225 | 0.07 | Bad. Correlation too low, data cannot be used. |
| MA02 | 45 - 240 | 1.7 | Good. |
| MAB03 | 230 | 1.3 | Bad. Correlation too low, data cannot be used. |
| MB02 | 140 - 315 | 1.7 | Good |
| MB01 | 150 - 280 | 0.3 | Good. Except pressure sensor (water levels). |
| MAB03 | 150 - 225 | 1.15 | Good. Except pressure sensor (water levels). |
| MB01 | 110 - 270 | 0.3 | Good. Except pressure sensor (water levels). |
| MB01 | 150 - 290 | 2.0 | Good. Except pressure sensor (water levels). |
| MB01 | 140 - 330 | 1.2 | Good. |

### 3.2.1. WATER LEVELS

The water levels are measured at the different measurement locations, and calculated with the data collected by the pressure sensors of the ADVs. As mentioned before the data from only one ADV shows reasonable results. This is the ADV situated at measurement location MA02 (*Sonneratio* patch) at 24 March and 5 April 2015 and situated at measurement location MB02 (tidal creekbank) at 25 March and 6 April 2015. The water levels increase fast during the incoming tidal flux and the water levels slowly decrease during the outgoing tidal flux (Fig. 17), this process is described in several studies (e.g. Furukawa et al. 1996).
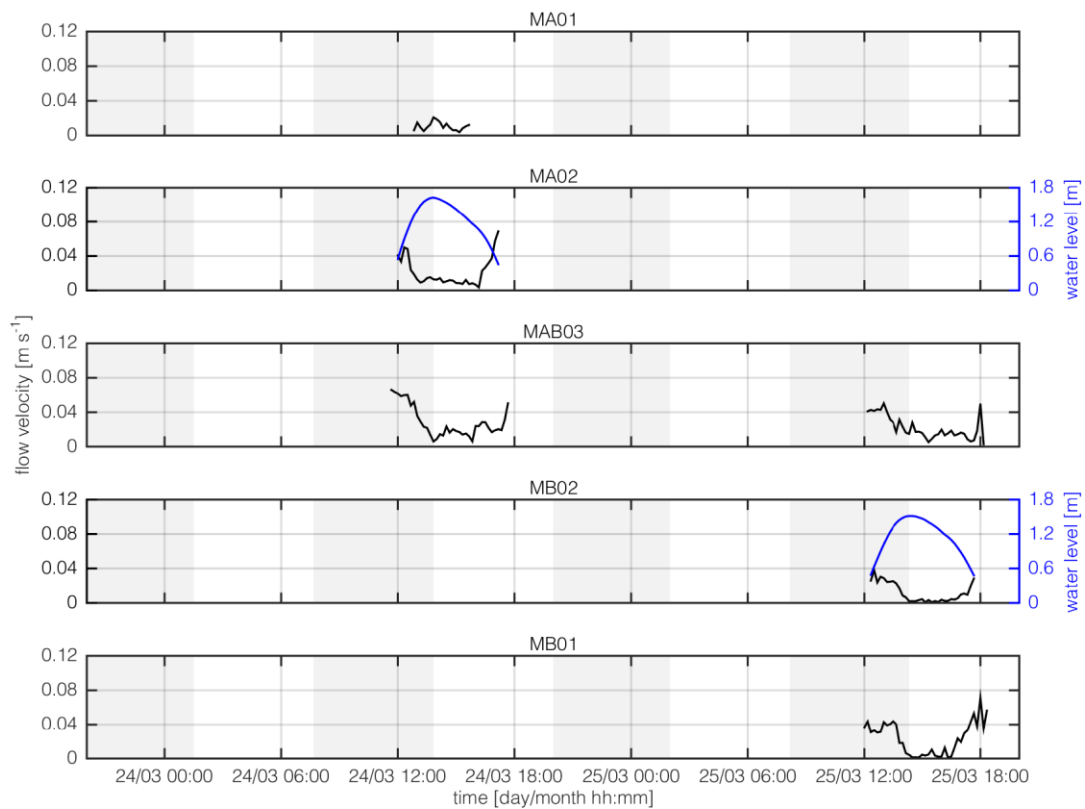
**FIGURE 17. FLOW VELOCITIES (BLACK) AND WATERLEVELS (BLUE) MEASURED AT 24 AND 25 MARCH 2015 AT THE DIFFERENT MEASUREMENT LOCATIONS MA01 (BACK OF THE FOREST), MA02 (*SONNERATIA* PATCH), MAB03 (MUDFLAT), MB02 (TIDAL CREEKBANK) AND MB01 (TIDAL CREEK).**

### 3.2.2. FLOW VELOCITY

Flow velocity data is measured with the same equipment at similar locations and periods as the water levels. The resulting flow velocities show a peak during ebb tidal current and in general a relative smaller peak during the sluggish flood tidal current, both related to the water levels (Fig. 17).

### 3.2.3. PROFILE DATA

Profile data shows data (water levels, flow velocities, flow directions and SSCs) at multiple heights in the same temporal scale, measured by three separate ADVs (Fig. 18). The water levels indirectly measured by the different ADVs show the characteristic deviations, the blue ADV shows the actual water levels (Fig. 18, panel 1). The flow velocity (Fig. 18, panel 2) is highest at the top of the profile, both during the ebb tidal wave and flood tidal wave, and lowest at the bottom, showing a typical vertical pattern. The other collected data (Fig. 18, panel 3 and 4), does not show clear patterns over the profile.

The flow velocity profiles at the different adjacent time steps of measurements related to the water levels, show a fragmented pattern (Fig. 19). When looking more specific to the parts from zero to the maximum flow velocity, from the maximum flow velocity to the minimum flow velocity and from the minimum flow velocity to zero flow velocity over time, the patterns still are fragmented.
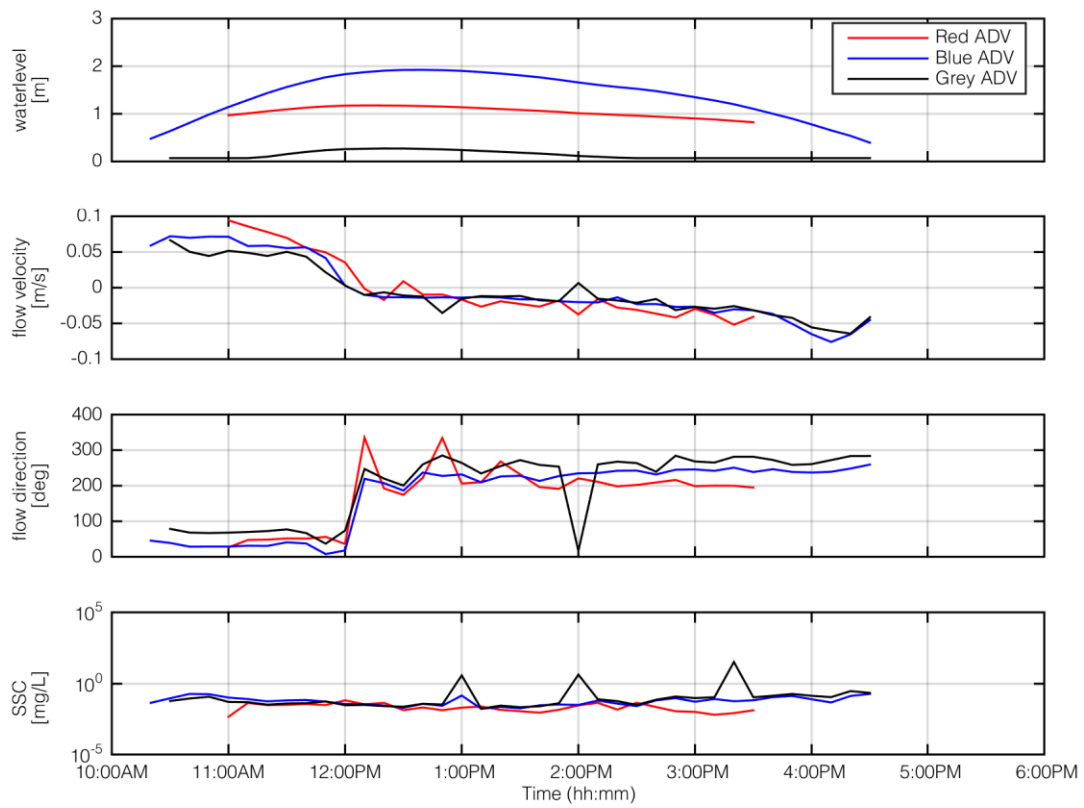
**FIGURE 18. DATA COLLECTED AND PROCESSED AT THREE DIFFERENT HEIGHTS: 7 CM (GREY), 22 CM (BLUE), 92 CM (RED), IN THE TIDAL CREEK (MB01).**
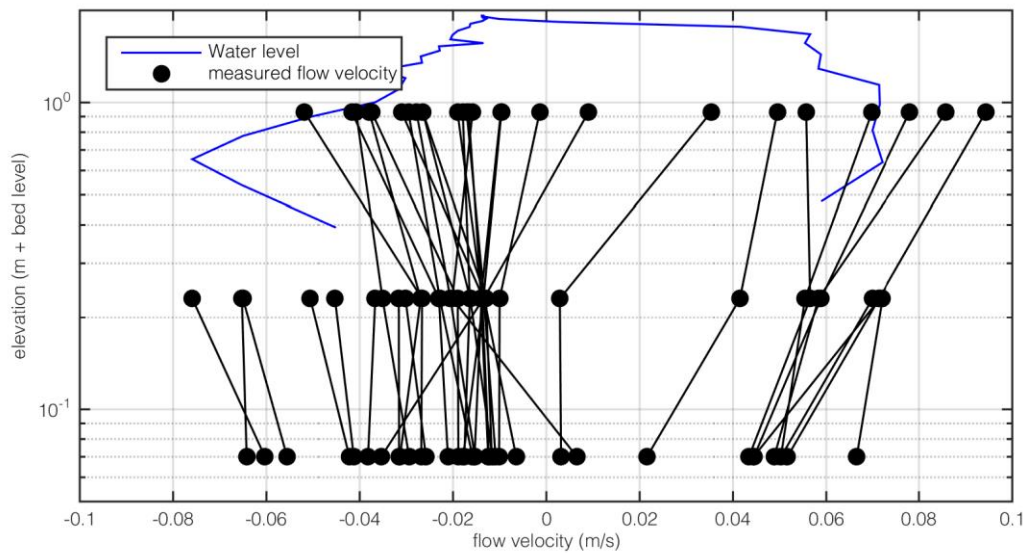


**FIGURE 19. FLOW VELOCITIES AT THE THREE MEASURED ELEVATION LEVELS.**

## 3.3.    SEDIMENT DEPOSITION

The sediment deposition shows a characteristic gradient from the front of the mangrove (high deposition) to the back of the mangrove (low deposition) (Fig. 20A). The measured deposition at the nearby locations MB01 and MB02 are almost equal, including the standard deviations, building confidence. The standard deviation are quite high, probably due to the deviating tidal waves, large particles on the trap and the small animals (e.g. snails) on the trap.
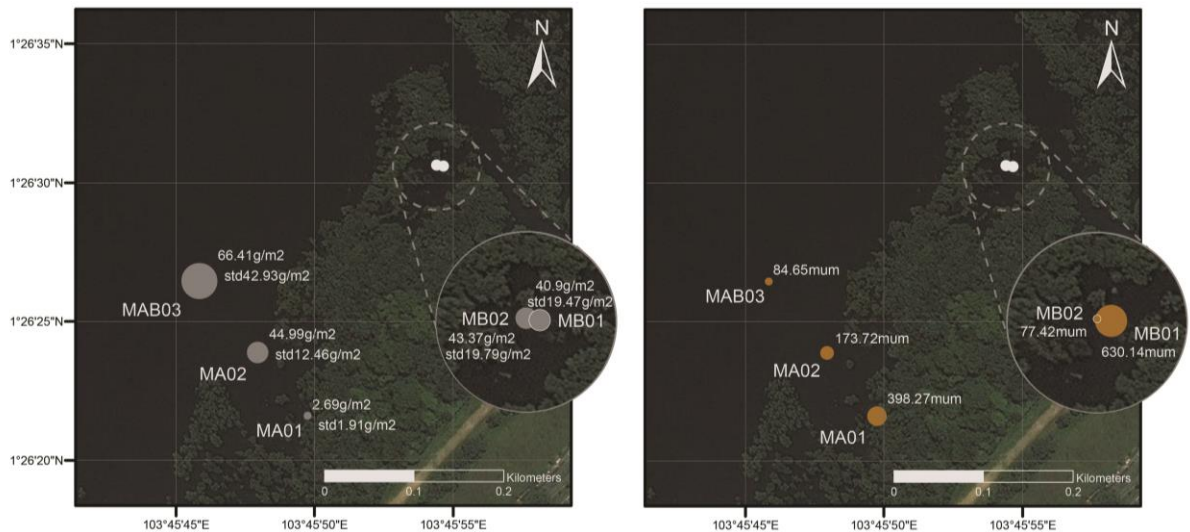


**FIGURE 20. LEFT TO RIGHT: (A) DEPOSITED SEDIMENT [g m$^{-2}$] WITH THE ASSOCIATED STANDARD DEVIATION [g m$^{-2}$] AT THE DIFFERENT MEASUREMENT LOCATIONS, AVERAGED OVER ALL MEASUREMENTS. (B) SPATIAL DISTRIBUTION OF GRAIN SIZES [d$_{50}$].**

## 3.4.    SEDIMENT CONCENTRATIONS

The measured and processed suspended sediment concentrations (Fig. 21) show fragmented results, the concentrations are highly deviating at the different measurement locations. In general it can be stated that during the measurement period there is a high concentration at the initial part of the incoming tidal flux, this decreases during the period the mangrove is inundated. When looking to the Mandai transect (MA01 – MA02 – MAB03), the concentrations are relative high in front of the mangrove and decreasing to the back of the mangrove. This pattern shows similarities with the sediment deposition (Fig. 20A).
Low SSC values in the back of the mangrove probably occur due to the low flow velocities. The transparency of the water in the field matches with the findings.
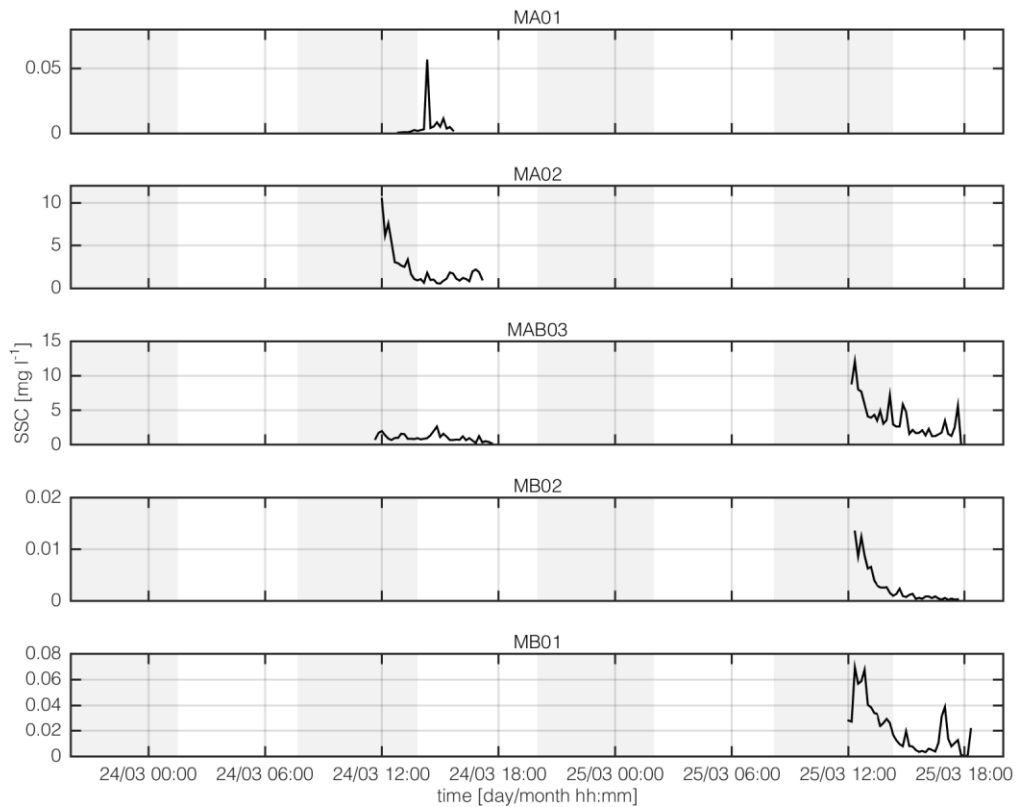
**FIGURE 21. SSC VALUES MEASURED AT 24 AND 25 MARCH 2015 AT THE DIFFERENT MEASUREMENT LOCATIONS MA01 (BACK OF THE FOREST), MA02 (*SONNERATIA* PATCH), MAB03 (MUDFLAT), MB02 (TIDAL CREEKBANK) AND MB01 (TIDAL CREEK). NOTE: THE LIMITS OF THE Y-AXIS ARE NOT EQUAL IN ALL PANELS**

## 3.5. SEDIMENT CHARACTERISTICS

Sediment characteristics are averaged over two measurements. The $d_{50}$ (table 11) shows an increasing pattern from the front of the mangrove to the back of the mangrove (Fig. 20B). The grain size distribution (Fig. 22) shows a high amount of clay and silt particles in the center of the mangrove (MA02, MAB03, MB02) and larger grain sizes in the tidal creek, where flow velocities are higher and at the back of the mangrove. The organic matter content (table 11) is highest in the center of the mangrove and in front of the mangrove (MA02, MAB03 and MB02), similar to other studies (e.g. Horstman et al. 2015) and lower values can be found at the back of the mangrove and in the tidal creek.

**TABLE 11. RESULTING D50 (µm) AND ORGANIC MATTER CONTENT OF THE SOIL SAMPLES AT THE DIFFERENT LOCATIONS**

| Location | Mean grain size, $d50\ [\mu m]$ | Organic matter content [%] |
|---|---|---|
| **MA01** | $3.83 \cdot 10^{2}$ | 2.94 |
| **MA02** | $4.40 \cdot 10^{1}$ | 15.21 |
| **MAB03** | $3.89 \cdot 10^{1}$ | 10.58 |
| **MB02** | $2.73 \cdot 10^{1}$ | 15.74 |
| **MB01** | $6.49 \cdot 10^{2}$ | 1.50 |
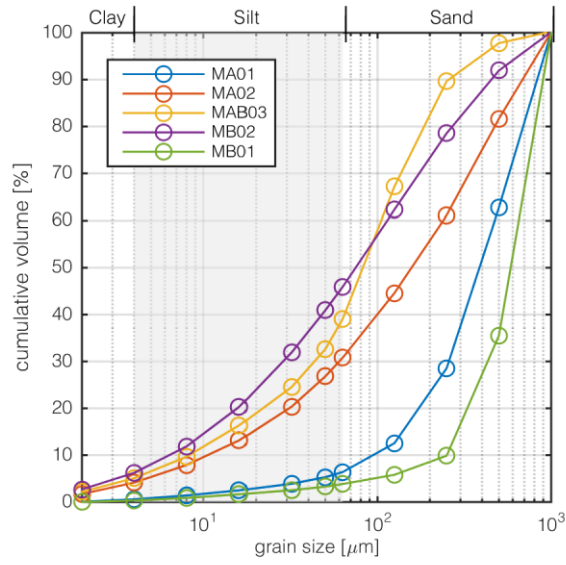
**FIGURE 22. GRAIN SIZE DISTRIBUTION AT THE DIFFERENT MEASUREMENT LOCATIONS MA01 (BACK OF THE FOREST), MA02 (SONNERATIA PATCH), MAB03 (MUDFLAT), MB02 (TIDAL CREEKBANK) AND MB01 (TIDAL CREEK).**

# 4. REFERENCES

Chanson, H., M. Takeuchi and M. Trevethan (2008). "Using turbidity and acoustic backscatter intensity as surrogate measures of suspended sediment concentration in a small subtropical estuary." Journal of Environmental Management **88**: 1406-1416.

Chanson, H., M. Trevethan and S. Aoki (2008). "Acoustic Doppler velocimetry (ADV) in small estuary: Field experience and signal post-processing." Flow Measurement and Instrumentation **19**(5): 307-313.

Costanza, R., R. d'Arge, R. d. Groot, S. Farber, M. Grasso, B. Hannon, K. Limburg, S. Naeem, R. V. O'Neill and J. Paruelo (1998). "The value of the world's ecosystem services and natural capital."

de Groot, R., L. Brander, S. van der Ploeg, R. Costanza, F. Bernard, L. Braat, M. Christie, N. Crossman, A. Ghermandi, L. Hein, S. Hussain, P. Kumar, A. McVittie, R. Portela, L. C. Rodriguez, P. ten Brink and P. van Beukering (2012). "Global estimates of the value of ecosystems and their services in monetary units." Ecosystem Services **1**(1): 50-61.

Friess, D. A., K. W. Krauss, E. M. Horstman, T. Balke, T. J. Bouma, D. Galli and E. L. Webb (2012). "Are all intertidal wetlands naturally created equal? Bottlenecks, thresholds and knowledge gaps to mangrove and saltmarsh ecosystems." Biological reviews **87**: 346-366.

Friess, D. A., J. Phelps, R. C. Leong, W. K. Lee, A. K. S. Wee, N. Sivasothi, R. R. Y. Oh and E. L. Webb (2012). "Mandai mangrove, Singapore: Lessons for the conservation of Southeast Asia's mangroves." The Raffles Bulletin of Zoology(25): 55-65.

Furukawa, K. and E. Wolanski (1996). "Sedimentation in Mangrove Forests." Mangroves and Salt Marshes **1**(1): 3-10.

Ha, H. K., W. Y. Hsu, J. P. Y. Maa, Y. Y. Shao and C. W. Holland (2009). "Using ADV backscatter strength for measuring suspended cohesive sediment concentration." Continental Shelf Research **29**(10): 1310-1316.

Hasan, G. M. J., D. S. van Maren and H. F. Cheong (2012). "Improving hydrodynamic modeling of an estuary in a mixed tidal regime by grid refining and aligning." Ocean Dynamics **62**(3): 395-409.

Hong, P. N. and H. T. San (1993). Mangroves of Vietnam. Bangkok, Thai.

Horstman, E. M. (2013). Bio-Physical interactions in coastal mangroves: data report - field campaign Trang, Thailand - Nov 2010/May 2011. Enschede, The Netherlands, University of Twente, CE&M research report.

Horstman, E. M. (2014). The mangrove tangle, short-term bio-physical interactions in coastal mangroves. Enschede, University of Twente.

Horstman, E. M., T. Balke, T. J. Bouma, C. M. Dohmen-Janssen and S. J. M. H. Hulscher (2011). Optimizing methods to measure hydrodynamics in coastal wetlands: evaluating the use and positioning of ADV, ADCP and HR-ADCP. Coastal Engineering 2010, Shanghai, China, Coastal Engineering Research Council.

Horstman, E. M., C. M. Dohmen-Janssen, T. J. Bouma and S. J. M. H. Hulscher (2015). "Tidal-scale flow routing and sedimentation in mangrove forests: Combining field data and numerical modelling." Geomorphology **228**(0): 244-262.

Horstman, E. M., C. M. Dohmen-Janssen and S. J. M. H. Hulscher (2013). "Flow routing in mangrove forests: A field study in Trang province, Thailand." Continental Shelf Research **71**(0): 52-67.

Hsiang, L. L. (2000). "Mangrove conservation in Singapore: A physical or a psychological impossibility?" Biodiversity & Conservation **9**(3): 309-332.

Kernkamp, H. W. J., H. A. H. Petit, H. Gerritsen and E. D. de Goede (2005). "A unified formulation for the three-dimensional shallow water equations using orthogonal co-ordinates: theory and application." Ocean Dynamics **55**(3-4): 351-369.

Kirwan, M. L. and P. Megonigal (2013). "Tidal wetland stability in the face of human impacts and sea-level rise." Nature **504**: 53-60.

Kurniawan, A., S. K. Ooi, S. Hummel and H. Gerritsen (2011). "Sensitivity analysis of the tidal representation in Singapore Regional Waters in a data assimilation environment." Ocean Dynamics **61**(8): 1121-1136.

Lee, W. K. (2014). "Unpublished data."

Mazda, Y., E. Wolanski and P. V. Ridd (2007). The role of physical processes in mangrove environments: manual for the preservation and utilization of mangrove ecosystems, Terrapub.

Nortek (2005). Vector Current Meter User Manual. Norway, Nortek.

Robertson, A. I. and D. M. Alongi (1992). Tropical mangrove ecosystems, American Geophysical Union.

Salehi, M. and K. Strom (2011). "Using velocimeter signal to noise ratio as a surrogate measure of suspended mud concentration." Continental Shelf Research **31**(9): 1020-1032.

SonTek (1997). Pulse Coherent Doppler Processing and the ADV Correlation Coefficient. San Diego, SonTek.

Syvitski, J. P. M., C. J. Vörösmarty, A. J. Kettner and P. Green (2005). "Impact of Humans on the Flux of Terrestrial Sediment to the Global Coastal Ocean." science **308**(5720): 376-380.

Thampanya, U., J. E. Vermaat, S. Sinsakul and N. Panapitukkul (2006). "Coastal erosion and mangrove progradation of Southern Thailand." Estuarine, Coastal and Shelf Science **68**(1–2): 75-85.

Valiela, I., J. L. Bowen and J. K. York (2001). "Mangrove Forests: One of the World's Threatened Major Tropical Environments." BioScience **51**(10): 807-815.

Van Maanen, B., G. Coco and K. R. Bryan (2015). On the ecogeomorphological feedbacks that control tidal channel network evolution in a sandy mangrove setting.

Van Santen, P., P. G. E. F. Augustinus, B. M. Janssen-Stelder, S. Quartel and N. H. Tri (2007). "Sedimentation in an estuarine mangrove system." Journal of Asian Earth Sciences **29**(4): 566-575.

Voulgaris, G. and S. T. Meyers (2004). "Temporal variability of hydrodynamics, sediment concentration and sediment settling velocity in a tidal creek." Continental Shelf Research **24**(15): 1659-1683.

Wolanski, E., S. Spagnol, S. Thomas, K. Moore, D. M. Alongi, L. Trott and A. Davidson (2000). "Modelling and Visualizing the Fate of Shrimp Pond Effluent in a Mangrove-fringed Tidal Creek." Estuarine, Coastal and Shelf Science **50**(1): 85-97.

Yee, A. T. K., W. F. Ang, S. Teo, S. C. Liew and H. T. W. Tan (2010). "The present extent of mangrove forests in Singapore." Nature in Singapore **3**: 139-145.